Published in final edited form as:

Mol Biochem Parasitol. 2017 September ; 216: 5–13. doi:10.1016/j.molbiopara.2017.06.002.

The *Plasmodium falciparum* exported protein PF3D7_0402000 binds to erythrocyte ankyrin and band 4.1

Bikash Shakya[1], **Wesley D. Penn**[1], **Ernesto S. Nakayasu**[2,3], and **Douglas J. LaCount**[1,*]

[1]Department of Medicinal Chemistry and Molecular Pharmacology, Purdue University, West Lafayette, IN 47907, U. S. A

[2]Bindley Bioscience Center - Discovery Park, Purdue University, West Lafayette, IN 47907, U. S. A

[3]Biological Sciences Division, Pacific Northwest National Laboratory, Richland, WA 99352, U. S. A

Abstract

Plasmodium falciparum extensively modifies the infected red blood cell (RBC), resulting in changes in deformability, shape and surface properties. These alterations suggest that the RBC cytoskeleton is a major target for modification during infection. However, the molecular mechanisms leading to these changes are largely unknown. To begin to address this question, we screened for exported *P. falciparum* proteins that bound to the erythrocyte cytoskeleton proteins ankyrin 1 (ANK1) and band 4.1 (4.1R), which form critical interactions with other cytoskeletal proteins that contribute to the deformability and stability of RBCs. Yeast two-hybrid screens with ANK1 and 4.1R identified eight interactions with *P. falciparum* exported proteins, including an interaction between 4.1R and PF3D7_0402000 (PFD0090c). This interaction was first identified in a large-scale screen (Vignali et al., Malaria J, 7:211, 2008), which also reported an interaction between PF3D7_0402000 and ANK1. We confirmed the interactions of PF3D7_0402000 with 4.1R and ANK1 in pair-wise yeast two-hybrid and co-precipitation assays. In both cases, an intact PHIST domain in PF3D7_0402000 was required for binding. Complex purification followed by mass spectrometry analysis provided additional support for the interaction of PF3D7_0402000 with ANK1 and 4.1R. RBC ghost cells loaded with maltose-binding protein (MBP)-PF3D7_0402000 passed through a metal microsphere column less efficiently than mock- or MBP-loaded controls, consistent with an effect of PF3D7_0402000 on RBC rigidity or membrane stability. This study confirmed the interaction of PF3D7_0402000 with 4.1R in multiple independent assays, provided the first evidence that PF3D7_0402000 also binds to ANK1, and suggested that PF3D7_0402000 affects deformability or membrane stability of uninfected RBC ghosts.

*Corresponding author. Department of Medicinal Chemistry and Molecular Pharmacology, Purdue University, RHPH 410A, 575 Stadium Mall Drive, West Lafayette, IN 47907, U.S.A., 765-496-7835, dlacount@purdue.edu.

Keywords

Plasmodium; exported protein; PF3D7_0402000; ankyrin; band 4.1; host-pathogen interaction

1 Introduction

Plasmodium falciparum infection of red blood cells (RBCs) leads to marked changes in shape, permeability, deformability and binding properties. Together these alterations create an environment that supports parasite replication, but also contribute to malaria pathogenesis [1]. The changes are attributed to the export of hundreds of proteins by the parasite to the infected RBC (iRBC) [2]. Although protein export is essential for parasite replication [3], the molecular targets and functions of the *P. falciparum* exported proteins are largely undefined. A subset of the exported proteins, are known to target the RBC cytoskeleton, including Knob associated histidine rich protein (KAHRP) [4, 5], Ring infected erythrocyte surface antigen (RESA) [6–8], Mature erythrocyte surface antigen (MESA) [9–11], *P. falciparum* erythrocyte membrane protein 3 (*Pf*EMP3) [12], Lysine-rich membrane-associated PHISTb protein (LyMP) [13], and *P. falciparum* protein 332 (Pf332) [14]. However, given the large number of exported proteins and the importance of the RBC cytoskeleton, it is likely that additional *P. falciparum* proteins also bind to erythrocyte cytoskeleton proteins.

The erythrocyte cytoskeleton is a flexible network based on spectrin dimers that are linked to each other and to the cell membrane via two multiprotein assemblies, the junctional and ankyrin complexes [15, 16]. In the junctional complex, six spectrin dimers bind to a short actin filament that is associated with accessory proteins tropomyosin, tropomodulin, adducin, and dematin. Band 4.1 (4.1R) facilitates the interaction between spectrin and actin, and provides links to the cell membrane through its interactions with the anion exchange channel (band 3) and glycophorin C (GPC). The 4.1R FERM (Four-point-one, Ezrin, Radixin, Moesin) domain interacts with p55, band 3 and GPC, whereas 4.1R C-terminal region binds to the actin-spectrin network [17–19]. Through its protein-protein interactions, 4.1R regulates local cell shape and contributes to the elasticity and mechanical stability of the RBC membrane [20–22].

Erythrocyte ankyrin (ANK1) is the key component to the ankyrin complex, linking spectrin to erythrocyte membrane proteins band 3 and RhAG [23, 24]. ANK1 has three domains: the N-terminal membrane-binding domain (MBD), the central spectrin binding domain, and the C-terminal regulatory domain. The MBD consists of 24 copies of the 33-amino acid ankyrin repeat which mediate binding to band 3 and several other proteins [15, 25, 26]. Similarly, the spectrin-binding domain directly interacts with repeats 14–15 of β-spectrin through the small ZU5A subdomain (zona occludens 1 (ZO-1) protein/unc5-like netrin receptor domain) [27, 28].

The critical location and functions of ANK1 and 4.1R make them prime targets for *P. falciparum* exported proteins. However, only a few parasite protein partners are known [10, 29–33]. Here, we hypothesize that additional *P. falciparum* exported proteins also target ANK1 and 4.1R. To test the hypothesis, we used ANK1 and 4.1R constructs as baits to

screen a *P. falciparum* cDNA library using the yeast two-hybrid assay. We identified eight proteins that reproducibly interacted with either ANK1 or 4.1R, and showed that one of these, PF3D7_0402000 (previous name, PFD0090c; referred to as D90c in figures), targeted both. We confirmed the interactions of PF3D7_0402000 in multiple independent assays, localized the binding regions on 4.1R, ANK1 and PF3D7_0402000, and provided evidence that PF3D7_0402000 can alter the deformability or stability of uninfected erythrocyte ghosts.

2 Methods

2.1 Yeast two-hybrid (Y2H) assays

PCR primers used in this study are listed in Supplementary Table 1. 4.1R and ANK1 gene fragments were PCR-amplified and cloned into the DNA binding domain (DBD) plasmid pOBD2 by homologous recombination in the yeast strain R2HMet (*MATa ura3-52 ade2-101 trp1-901 leu2-3,112 his3-200 met2Δ::hisG gal4Δ gal80Δ*). Following the verification by PCR and sequencing, the DBD fusion proteins were tested for self-activation by growth on histidine-deficient medium with increasing concentrations of 3-amino-1,2,4-triazole (3-AT) (Sigma) [34, 35]. The lowest 3-AT concentration that prevented yeast growth was used for the Y2H assays. Y2H screens were performed as described previously [34, 36] by mating the DBD-expressing strains with yeast strain BK100 (*MATa ura3-52 ade2-101 trp1-901 leu2-3,112 his3-200 gal4Δ gal80Δ GAL2-ADE2 LYS2::GAL1-HIS3 met2::GAL7-lacZ*) containing a *P. falciparum* Y2H library cloned into the activation domain (AD) plasmid pOAD102 [34, 37]. Y2H positive colonies were selected on synthetic defined (SD) medium lacking tryptophan, leucine, uracil, and histidine, and containing 3-AT at the concentration determined above (SD–TLUH + 3-AT). *P. falciparum* gene fragments from colonies that grew on SD–TLUH + 3-AT were PCR-amplified, sequenced, and identified using BlastN to query the *P. falciparum* open reading frames (ORFs) in PlasmoDB [38].

Pair-wise Y2H assays were performed by mating strains expressing DBD and AD fusion proteins and selecting for diploid colonies on SD medium lacking tryptophan and leucine. Diploid strains were grown in liquid media, adjusted to an OD_{600} = 1.0, serially diluted five-fold, and plated on SD–TLUH plus 3-AT as described above. Additional experiment-specific details can be found in the figure legends.

2.2 SDS-PAGE and western blotting

Samples were mixed with Laemmli SDS-PAGE sample buffer containing 5% β-mercaptoethanol, boiled for 5 min, subjected to SDS-PAGE on 10% polyacrylamide gels and transferred to nitrocellulose membranes. Membranes were probed sequentially with primary and HRP-conjugated secondary antibodies, and visualized with enhanced chemiluminescence (ECL) western blotting reagent (Pierce).

2.3 Co-purification assays

A fragment of PF3D7_0402000 encoding amino acids 85–297 was cloned into a modified pMAL-c4e vector that incorporated a hexahistidine (6×His) tag at the 3′ end. Maltose binding protein (MBP)-His6 (hereafter referred to as MBP-His) and MBP-PF3D7_0402000-

His6 (hereafter referred to as MBP-D90c-His) were overexpressed in the *E. coli* Rosetta (DE3) pLysS cells (Novagen) and affinity purified with TALON® metal affinity resin (Clontech) as described previously [39]. Fusion proteins were eluted in PBS containing 300 mM imidazole and 100 μM PMSF. For pull-down assays, equimolar amounts of MBP-His and MBP-D90c-His were incubated with amylose resin (New England BioLabs) overnight at 4° C with rotation, washed with PBS containing 100 μM PMSF and 0.5 % Triton X-100 (Alfa Aesar), and distributed to individual tubes. Putative binding partners or control proteins were *in-vitro* translated in wheat germ extracts (Promega) as fusions to three copies of the FLAG epitope tag (3XFLAG) and the C-terminal fragment of firefly luciferase (C-FLuc). Equivalent amounts of the *in vitro* translated proteins were added to each binding reaction, incubated for 4 hours at 4° C with rotation, washed three times, eluted by boiling in Laemmli SDS-PAGE sample loading buffer, and subjected to western blot analysis. Glutathione S-transferase (GST) pull-down assays were performed with GST or GST-tagged PF3D7_0402000 (GST-D90c) that was *in vitro* translated using wheat germ extracts [40]. GST or GST-D90c were mixed with 3XFLAG-C-FLuc tagged ANK1 and 4.1R, incubated with GST beads (Thermo Scientific) overnight at 4° C in presence of protease inhibitor (PI) cocktail (Roche), washed three times with PBS+0.1% TritonX-100, eluted by boiling in Laemmli SDS-PAGE sample loading buffer, and subjected to western blot analysis.

2.4 Inside-out vesicle (IOV) binding assay

RBC ghosts and IOVs were prepared from fresh human blood (BioChemed, Winchester, VA) as described [39]. 3XFLAG-tagged PF3D7_0402000 (3XFLAG-D90c) was added to 20 μl IOVs, diluted to a final volume of 150 μl with PBS, 2% BSA plus PI cocktail, and incubated overnight on ice with occasional mixing. IOVs were collected by centrifugation at 3700 × g for 30 min at 4° C, washed twice with cold PBS containing 0.25 mM KCl, resuspended in Laemmli SDS-PAGE sample loading buffer and processed for western blot analysis.

2.5 Co-affinity purification of PF3D7_0402000-binding proteins from erythrocyte extracts

Purified MBP-D90c-His and MBP-His were used for the co-affinity purification of proteins from erythrocyte extracts. To prepare a soluble extract of erythrocyte cytoskeletal proteins, RBC ghosts were suspended in 1 M KCl, 0.5 M sodium phosphate (pH 8.0) supplemented with PI cocktail and incubated on ice for 2 h with occasional mixing. Insoluble material was pelleted by centrifugation at 210,000 × g for 30 min at 4° C. The supernatant, which contained solubilized RBC cytoskeletal membrane proteins, was collected and dialyzed against PBS overnight. Solubilization of RBC cytoskeletal proteins was confirmed by subjecting the supernatant and the pellet to SDS-PAGE followed by staining with Coomassie Blue.

Amylose beads (40 μl) were equilibrated in amylose wash buffer (1XPBS, PI, 100 μM PMSF and 0.5% Triton X-100), mixed with 250 μg MBP-D90c-His or MBP-His and incubated at 4° C with rotation for 4 hours. After collecting the beads by centrifugation at 700 × g for 2 minutes, 450 μl of RBC cytoskeletal extract was added. Beads were incubated overnight at 4° C with rotation and washed 4 times with 40 volumes of amylose wash buffer

for 10 min with rotation per wash. Proteins associated with the amylose beads were eluted twice with 150 μl of PBS containing PI, 20 mM maltose and 100 μM PMSF.

2.6 Sample preparation and liquid chromatography-tandem mass spectrometry (LC-MS/MS) analysis

The soluble RBC cytoskeletal protein lysate and proteins from the co-purification assays were precipitated by adding 3 volumes of ice-cold acetone and incubating overnight at −20° C. Precipitated proteins were collected by centrifugation at 16,000 × g for 20 min at 4° C, washed with cold acetone and dried in fume hood for 1–2 h. The dried pellet was dissolved in 20 μl of 50 mM NH_4HCO_3 containing 8 M urea and disulfide bonds were reduced with 10 mM dithiothreitol (DTT) at 37° C for 1h. After cooling to room temperature, cysteine residues were alkylated by adding 2 μL of 400 mM iodoacetamide and incubating at 37° C in the dark for 1 h. Proteins were digested overnight at 37° C by adding 140 μL of 3.5 ng/μL trypsin dissolved in a buffer containing 50 mM NH_4HCO_3 and 1.3 mM $CaCl_2$. The digested peptides were loaded onto C18 microspin columns; centrifuged according to the manufacturer's instructions; the column was equilibrated by flushing twice with 100 μL of 100 % methanol and twice with 100 μL of 0.1 % trifluoroacetic acid (TFA), then the sample was loaded and the column was washed three times with 100 μL of 5 % acetonitrile (ACN)/ 0.1 % TFA before eluting the peptides in 100 μL 80% ACN/0.1% TFA [41, 42]. After drying in a SpeedVac, the samples were resuspended in 20 μL 0.1% formic acid and stored at −20° C. Samples were subjected to LC-MS/MS analysis on an NanoAcquity UPLC (Waters) connected to a Q Exactive Plus mass spectrometer (Thermo Fisher Scientific). Peptides were loaded into a C18 trap column (5 cm × 360 μm OD × 150 μm ID fused silica capillary tubing, Polymicro, Phoenix, AZ; packed with 3.6-μm Aeries C18 particles, Phenomenex, Torrence, CA) and separated in a capillary C18 column (70 cm × 360 μm OD × 75 μm ID packed with 3-μm Jupiter C18 stationary phase, Phenomenex) with the following gradient: 1–8% B solvent in 2 min (Solvent A: 0.1% FA in water and solvent B: 0.1% FA in acetonitrile), 8–12% B in 18 min, 12–30% B in 55 min, 30–45% B in 22 min, 45–95% B in 3 min, hold for 5 min in 95% B and 99–1% B in 10 min. The flow rate was set at 300 nL/min and the eluting peptides were directly analyzed by electrospray ionization. MS scans were collected in the range of 400 to 2000 m/z a resolution of 35,000 at m/z 400. The top 12 most intense parent ions ≥ 2 charges were submitted to high-collision energy (HCD) fragmentation once with normalized collision energy of 30 and resolution of 17,000 at m/z 400, before dynamically excluding it for 30 s.

LC-MS/MS data were submitted to database searches using MaxQuant version 1.5.5.1 [43] against a sequence FASTA file containing human and *Plasmodium falciparum* 3D7 proteins (downloaded from Uniprot Knowledge Base on November 11, 2014). The search parameters considered fully tryptic digestion with two missed cleavages allowed, protein N-terminus acetylation and methionine oxidation as variable modifications, and cysteine carbamidomethylation as fixed modification. The parent mass tolerance was set at 20 and 4.5 ppm for the first and second searching rounds. The results were filtered at 1% false-discovery rate at both protein and peptide-spectrum match levels. Quantitative analysis was performed by spectral counting and the significantly enriched proteins in the affinity

purifications were determined by the Significance Analysis of the INTeractome (SAINT) [44, 45].

2.7 Loading of MBP-His fusion proteins into erythrocyte ghosts

Erythrocyte ghosts were loaded with MBP-His fusion proteins and resealed as described [46]. Fresh human blood (BioChemed, Winchester, VA) was washed and resuspended in PBS-glucose containing 1 mM ATP at 50% hematocrit. The erythrocyte suspension was mixed with MBP-D90c-His6 or MBP-His6 and dialyzed against ATP containing hypotonic potassium buffer for 1 h at 4° C in prewetted 3.5-kDa molecular weight cut-off Slide-a-lyzer dialysis cassettes (Thermo Scientific). Lysed cells were removed from the cassette, combined with resealing buffer and incubated for 1 h at 37° C. Resealed ghosts were washed three times in RPMI medium and resuspended in complete RPMI medium containing 4% human serum and 0.125% Albumax (Gibco). Loading was confirmed by treatment with Proteinase K. Erythrocyte ghosts (2.5×10^7 cells) loaded with proteins were mock treated or treated with 100 μg/ml of Proteinase K (New England BioLabs), 0.5% Triton X-100 or both. After incubating 30 min at 37° C, protease activity was stopped by adding 1 mM PMSF. Proteins from 1×10^7 cells were solubilized in Laemmli SDS-PAGE sample loading buffer, separated by SDS-PAGE and immunoblotted using anti-MBP antibody (Santa Cruz), as previously described [46].

2.8 Microsphiltration assays

Microsphere filtration (microsphiltration) was performed as described [47]. Briefly, a matrix composed of calibrated microspheres with diameters of 5 to 15 μm and 15 to 25 μm (Type 5 and Type 6 solder powder with a composition of 96.50% tin, 3.00% silver, and 0.50% copper, Gesick MPM) was used to assess the deformability of parasite protein-loaded erythrocyte ghosts under flow. The suspension of microspheres in complete RPMI medium was loaded into 1 ml anti-aerosal filter pipet tip (Dot Scientific) and allowed to settle to form a 4–5 mm thick microsphere layer above the filter. Suspensions of protein loaded erythrocyte ghosts were layered onto microsphere column, perfused through the microsphere matrix at a flow rate of 60 ml/h using an electric pump (NE-1000, New Era Pump Systems), and washed with 6 ml of complete RPMI medium. The number of intact erythrocyte ghosts that passed through the microsphere matrix was counted on a hemocytometer. Statistical significance was determined using the Mann-Whitney U test implemented in GraphPad Prism software (version 6.0d).

3 RESULTS

3.1 Identification of *P. falciparum* exported proteins that bind to erythrocyte proteins ANK1 and 4.1R

To identify *P. falciparum* proteins that interacted with the RBC cytoskeletal proteins ANK1 and 4.1R, we performed Y2H screens of a *P. falciparum* cDNA library. Due to the large size of 4.1R and ANK1, each protein was expressed as smaller fragments to increase the likelihood of success in the Y2H (two for 4.1R and four for ANK1; Fig. 1A and B) [48]. The screens identified five interactions with the ANK1 and three with 4.1R that were recapitulated in pairwise Y2H assays in freshly transformed yeast (Table 1).

The interaction of PF3D7_0402000 with 4.1R was previously reported in a large-scale Y2H screen to identify human proteins that bound to *P. falciparum* proteins [33] and in a focused screen to identify *P. falciparum* binding partners of 4.1R [32]. The large-scale screen also suggested that PF3D7_0402000 interacted with a fragment of neuronal ankyrin (ANK2) that was similar to the ANK1 fragment (FG1, amino acids 1–497) used in this study [33]. The absence of PF3D7_0402000-ANK1 in our library screens with ANK1 was likely because some interactions can only be observed in the Y2H assay when particular combinations of binding domain and activation domain fusions are employed (for example, [49]).

To test if PF3D7_0402000 was able to bind to erythrocyte ankyrin, we performed a pairwise Y2H assay using PF3D7_0402000 as bait and 4.1R and ANK1 fragments as prey. PF3D7_0402000 interacted with both 4.1R and ANK1 as indicated by growth on Y2H selection medium (Fig. 1C). To determine if PF3D7_0402000 had the potential to bind to additional erythrocyte cytoskeletal proteins, we screened PF3D7_0402000 against a human bone marrow AD library. These screens also identified ANK1 and 4.1R as partners of PF3D7_0402000, but did not reveal any other RBC cytoskeletal proteins.

3.2 The PF3D7_0402000 PHIST domain is required for binding to ANK1

PF3D7_0402000 has a single known domain, the *Plasmodium* helical interspersed sub-telomeric (PHIST) domain (also referred to as the *Plasmodium RESA* N-terminal (PRESAN) domain; Pfam ID: PF09687). This domain is approximately 150 amino acids and is composed of 4 alpha helical regions [50–53]. In PF3D7_0402000 the PHIST domain resides between amino acids 150 and 300 and is flanked by low complexity regions. Parish et al. previously reported that PF3D7_0402000 PHIST domain was required for binding of PF3D7_0402000 [32]. To define the smallest region of PF3D7_0402000 that could bind to ANK1, a series of PF3D7_0402000 deletion constructs were tested in a pair-wise Y2H experiment (Fig. 2A). The smallest fragment from the deletion series that interacted with ANK1 was an N-terminal truncation of PF3D7_0402000 consisting of amino acids 137 – 297 (fragment 7), which encompassed the intact PHIST/PRESAN domain; this same fragment was also the smallest one that interacted with 4.1R (Fig. 2B). In contrast, no C-terminal truncations that disrupted the PHIST/PRESAN region were able to interact with either 4.1R or ANK1 (Fig. 2B). Thus, the PHIST domain is required for the interaction of PF3D7_0402000 with both ANK1 and 4.1R.

3.3 Confirmation of PF3D7_0402000 interactions in co-precipitation assays

To confirm the protein-protein interactions observed in Fig. 1 we used co-precipitation assays in two formats. PF3D7_0402000 lacking the N-terminal signal peptide, the export motif, and the C-terminal low complexity region was expressed in *E. coli* as a fusion to MBP-6XHis (MBP-D90c-His), purified, and incubated with *in vitro* translated, FLAG epitope-tagged ANK1 (amino acids 189–465) or 4.1R (Transcript variant 1, amino acids 210–664) (Fig. 3A). MBP-D90c-His, but not MBP-His, co-precipitated ANK1 and 4.1R (Fig. 3B). A FLAG-tagged negative control (the C-terminus of firefly luciferase) did not co-purify with either MBP-D90c-His or MBP-His. Similarly, *in vitro* translated FLAG-tagged ANK1 (amino acids 189–465) and 4.1R (Transcript variant 1, amino acids 210–664) co-purified with *in vitro* translated GST- PF3D7_0402000 but not GST (Fig. 3C and D). Thus,

ANK1 and 4.1R co-precipitated with PF3D7_0402000 under stringent washing conditions using two different affinity tags.

The ANK1 membrane binding domain is composed of 24 ankyrin repeats that form four folding domains (D1–4). The co-precipitation assays in Fig. 3 demonstrated that PF3D7_0402000 interacted with an ANK1 fragment that included the complete D2 domain (amino acids 205–402) and parts of the D1 and D3 domains [26]. Using co-precipitation assays individual ANK1 domains, we found that the ANK1 D2 domain was sufficient to interact with PF3D7_0402000 (Fig. 4).

3.4 PF3D7_0402000 binds to inside out vesicles (IOVs) prepared from red blood cells

The interaction of PF3D7_0402000 with 4.1R and ANK1 suggested that PF3D7_0402000 should bind to the erythrocyte cytoskeleton. To test this prediction, we used IOVs, which retain the erythrocyte cytoskeleton but expose the cytoskeletal components on the outside of vesicles [13, 39, 54]. Increasing concentrations of purified MBP-D90c-His or an MBP-MESA construct previously shown to bind to IOVs were incubated with a constant amount of freshly prepared IOVs [9, 10, 39]. Both PF3D7_0402000 and MESA bound to IOVs in a concentration dependent manner, confirming that PF3D7_0402000 targets a component of the erythrocyte cytoskeleton (Fig. 5). However, MESA bound to IOVs at lower concentrations than PF3D7_0402000 suggesting that MESA has a higher affinity for its target(s) than PF3D7_0402000.

3.5 PF3D7_0402000 co-precipitated 4.1R and ANK1 from erythrocyte cytoskeletal extracts

In an effort to further validate the interactions of PF3D7_0402000 with human erythrocyte cytoskeletal proteins, we performed affinity purification followed by mass spectrometry (AP-MS). PF3D7_0402000 was expressed as a fusion to MBP-His and incubated with a soluble cytoskeletal extract. As negative control, we included MBP-His. Complexes were purified on amylose beads, washed, eluted with biotin and subjected to liquid chromatography-mass spectrometry (LC-MS). Both PF3D7_0402000 and MBP-His tag were detected in their respective co-purification assays, confirming that the pull downs were successful. To distinguish true interactions from non-specific background, the LC-MS data was analyzed using the Significance Analysis of Interactome (SAINT) program [44, 45].

PF3D7_0402000 and 15 erythrocyte proteins were present in the MBP-PF3D7_0402000 co-precipitations at significantly higher levels relative to the MBP-His negative control (SAINT scores >0.9, Table 2). 4.1R and ANK1 were the most abundant erythrocyte proteins in the PF3D7_0402000 co-precipitations. Notably absent, however, were spectrin α and β, which link the junctional and ankyrin complexes. Without these bridging proteins, it is unlikely that ANK1 co-purified with PF3D7_0402000 via indirect interactions with 4.1R. In contrast, several other co-purifying erythrocyte proteins bind directly to 4.1R or ANK1, or indirectly via band 3, which binds to both ANK1 and 4.1R. These include band 3 (SLC4A1), glyceraldehyde 3-phosphate dehydrogenase (GAPDH), glucose transporter-1 (GLUT1/SLC2A1), 4.2R, dematin (DMTN), β-actin (ACTB), heat shock protein 70 (HSPA8) [55], α- and β-hemoglobin (HBA1 and HBB, respectively) and catalase (CAT) [55]. Of the remaining co-purifying erythrocyte proteins, argonaute 2 (AGO2) is perhaps the most

interesting due to its inclusion in exosomal vesicles released from *P. falciparum*-infected red blood cells [56, 57]. Other than ANK1 and 4.1R, none of the erythrocyte proteins that co-purified with PF3D7_0402000 were found in Y2H library screens.

3.6 PF3D7_0402000 reduced the deformability of erythrocyte ghosts

Multiple *P. falciparum* exported proteins targeting RBC cytoskeletal proteins influence the erythrocyte membrane stability or rigidity [7, 58–60]. Some of these proteins, such as RESA and PfEMP3, also bind directly to RBC cytoskeletal proteins [7, 12, 59, 61]. To investigate the effect of PF3D7_0402000 on the RBC cytoskeleton, we employed the microsphiltration assay, which uses a short column of metal microspheres to mimic the geometry of short and narrow inter-endothelial splenic slits, and thus models the mechanical challenges posed to RBCs by the human spleen [47, 61, 62]; this assay has been used in several studies to examine the contribution of *P. falciparum*-exported proteins to iRBC rigidity. iRBCs are passed through the metal microsphere matrix and the number of cells in the post-matrix ("downstream") sample are compared to the starting population.

Erythrocyte ghosts were loaded with purified and dialyzed MBP-D90c-His or MBP-His at a concentration of 30 μM and resealed in as described previously [46]. This concentration is within the range tested for RESA and PfEMP3 in similar assays [63, 64]. In sealed erythrocyte ghosts, the amount of MBP-D90c-His or MBP-His was predicted to exceed the amount of 4.1R and ANK1 by ~6 to 10-fold, assuming ~200,000 copies of 4.1R per cell, 120,000 copies of ANK1 per cell, and an average ghost cell volume of 66 fL [65, 66]. Successful loading was confirmed by demonstrating the proteins were protected from degradation by proteinase K (Fig. 6A) [46]. The resealed ghosts were passed through the microsphere matrix and the number of cells in the up- and downstream samples were counted. Passage of PF3D7_0402000-loaded ghosts through the microsphere matrix was significantly reduced compared to MBP-His- or mock-loaded ghosts (Fig. 6B), indicating that the presence of PF3D7_0402000 altered the cytoskeletal properties.

4 Discussion

PF3D7_0402000 is a PEXEL-containing, exported protein that is expressed at peak levels in trophozoites [67]. In infected cells, PF3D7_0402000 accumulated at the parasitophorous vacuole membrane (PVM), where it colocalized with 4.1R [32]. Deleting *PF3D7_0402000* had no effect on growth of the parasite in cell culture and yielded no obvious phenotypes [58]. A slight reduction in the rigidity of infected cells was observed, but was not statistically significant [58]. However, a proteomic analysis of field isolates from patients with cerebral or uncomplicated malaria found that PF3D7_0402000 was upregulated in cerebral malaria isolates relative to the uncomplicated malaria strains, possibly suggesting a more important role for PF3D7_0402000 in pathogenesis in humans [68].

In this study, we extended previous analyses of the erythrocyte targets of PF3D7_0402000 (PFD0090c) [32, 33]. Using multiple independent assays, we obtained further confirmation that *P. falciparum* PF3D7_0402000 interacts with 4.1R and provided the first evidence that PF3D7_0402000 binds to ANK1. Binding of PF3D7_0402000 to 4.1R and ANK1 was demonstrated in the Y2H assay (this report and [32, 33]), in pull down assays with *E. coli*-

expressed or *in vitro* translated proteins using different epitope or affinity tags, and by co-affinity purification plus mass spectrometry from erythrocyte cytoskeleton lysates. In both cases, an intact PHIST domain was required for the interaction. Similar to 4.1R, ANK1 has been reported to relocalize from the erythrocyte membrane to other sites during *P. falciparum* infection, primarily to Maurer's cleft but also to the PVM [69], where it would be available to bind to PF3D7_0402000.

Introducing PF3D7_0402000 into erythrocyte ghosts altered their membrane properties (Fig. 7). Ghost cells loaded with MBP-PF3D7_0402000-His passed through the microsphiltration column less efficiently than mock-treated erythrocytes or erythrocytes loaded with MBP-His. One explanation for this effect is that PF3D7_0402000 reduced the deformability of the erythrocyte ghosts. PF3D7_0402000 binds to the FERM domain of 4.1R [32], which also contains binding sites for erythrocyte membrane proteins band 3, glycophorin C and p55 [17–19, 21, 70, 71]. Disrupting the interaction between 4.1R and band 3 with the peptide IRRRY reduced the deformability of erythrocyte ghosts [72]. Thus, PF3D7_0402000 could reduce deformability by disrupting the interaction between band 3 and 4.1R in a similar manner.

Alternatively, the reduction in PF3D7_0402000-loaded erythrocyte ghosts in the downstream fraction of the microsphiltration experiment may be due to reduced membrane stability, leading to lysis when passed through the microsphere matrix under pressure. This is consistent with an effect of PF3D7_0402000 on the interactions of ANK1. PF3D7_0402000 bound to the D2 subdomain of ANK1 (Fig. 4), which contains a high affinity-binding site for band 3. Disrupting the band 3-ANK1 interaction reduced RBC membrane stability [73]. If PF3D7_0402000 has similar effect on the band 3-ANK1 interaction, the erythrocyte membrane could be destabilized, which would account for the results in our microphiltration experiments.

Since most PF3D7_0402000 was localized to the PVM in infected cells [32], the relevance of the effect of PF3D7_0402000 in uninfected erythrocyte ghosts is unclear. However, in the colocalization experiments of PF3D7_0402000 and 4.1R, little 4.1R was apparent at the periphery of the infected RBC [32], indicating that either 4.1R was nearly quantitatively extracted from the erythrocyte cytoskeleton or the immunofluorescence assays were not able to detect less dense labeling at the iRBC membrane. If the latter, it is possible that a subpopulation of PF3D7_0402000 may also be at the erythrocyte cytoskeleton.

PF3D7_0402000 was one of three PHIST domain proteins in this study that bound to either ANK1 or 4.1R (Table 1). PHIST is an ~150 amino acid domain that has undergone an expansion in *Plasmodium* [50]. Three subgroups (a, b, and c) have been described based on the patterns of conserved tryptophan residues [50]. Several PHISTb domain-containing parasite proteins traffic to the erythrocyte cytoskeleton [74]. Moreover, the PHISTb domain plus an N-terminal extension was sufficient to direct the PHISTb proteins to the iRBC membrane and to confer detergent insolubility [74], suggesting that the PHISTb domains bind to one or more erythrocyte cytoskeletal proteins. Consistent with this hypothesis, the two PHISTb domain proteins identified in this study, PF3D7_0902700 and PF3D7_1102500, bound to ANK1 and 4.1R, respectively, but at different domain than

PF3D7_0402000 (Table 1). In contrast, the PHISTa and PHISTc domain proteins tested by Tarr et al. were diffusely localized to the host cell cytosol or to punctate structures [74]. Similarly, PF3D7_0402000, a PHISTa protein, also does not appear to traffic to the erythrocyte periphery, but rather localizes to the PVM [32]. Although an intact PHIST domain was required for binding of PF3D7_0402000 to ANK1 and 4.1R (Fig. 2 and [32]), it is not known if this domain is sufficient for PVM localization. Both ANK1 and 4.1R are recruited to the PVM, and 4.1R colocalized with PF3D7_0402000 at this site [32]. However, our observation that PF3D7_0402000 stably associated with IOVs suggests PF3D7_0402000 is unable to liberate 4.1R or ANK1 from the cytoskeleton. Further studies will be needed to determine which other *P. falciparum* proteins contribute to ANK1 and 4.1R relocalization and to elucidate the binding potential of PHISTa, b and c domains.

Supplementary Material

Refer to Web version on PubMed Central for supplementary material.

Acknowledgments

We thank H. F. Brown, L. Wang and M. Burnet for assistance with experiments, and Dr. H. Choi (National University of Singapore) for help with the SAINT analysis. The authors acknowledge the use of the facilities of the Bindley Bioscience Center, a core facility of the NIH-funded Indiana Clinical and Translational Sciences Institute, and the national scientific user facility at the Environmental Molecular Sciences Laboratory, sponsored by the U.S. DOE OBER.

This work was supported by the National Institutes of Health [grant number R01GM092829] and the Indiana Clinical and Translational Sciences Institute, funded in part by grant #UL1 TR001108 from the National Institutes of Health, National Center for Advancing Translational Sciences, Clinical and Translational Sciences Award. B. S. was supported in part by a fellowship from the Purdue Research Foundation.

References

1. Starnes GL, Waters AP. Home improvements: how the malaria parasite makes the red blood cell home sweet home. J Mol Cell Biol. 2010; 2(1):11–3. [PubMed: 19805414]
2. de Koning-Ward TF, Dixon MW, Tilley L, Gilson PR. *Plasmodium* species: master renovators of their host cells. Nat Rev Microbiol. 2016; 14(8):494–507. [PubMed: 27374802]
3. Boddey JA, Carvalho TG, Hodder AN, Sargeant TJ, Sleebs BE, Marapana D, Lopaticki S, Nebl T, Cowman AF. Role of plasmepsin V in export of diverse protein families from the *Plasmodium falciparum* exportome. Traffic. 2013; 14(5):532–50. [PubMed: 23387285]
4. Kilejian A, Rashid MA, Aikawa M, Aji T, Yang YF. Selective association of a fragment of the knob protein with spectrin, actin and the red cell membrane. Mol Biochem Parasitol. 1991; 44:175–181. [PubMed: 2052019]
5. Taylor DW, Parra M, Chapman GB, Stearns ME, Rener J, Aikawa M, Uni S, Aley SB, Panton LJ, Howard RJ. Localization of *Plasmodium falciparum* histidine-rich protein 1 in the erythrocyte skeleton under knobs. Mol Biochem Parasitol. 1987; 25:165–174. [PubMed: 2444884]
6. Da Silva ED, Foley M, Dluzewski AR, Murray LJ, Anders RF, Tilley L. The *Plasmodium falciparum* protein RESA interacts with the erythrocyte cytoskeleton and modifies erythrocyte thermal stability. Mol Biochem Parasitol. 1994; 66:59–69. [PubMed: 7984188]
7. Pei X, Guo X, Coppel R, Bhattacharjee S, Haldar K, Gratzer W, Mohandas N, An X. The ring-infected erythrocyte surface antigen (RESA) of *Plasmodium falciparum* stabilizes spectrin tetramers and suppresses further invasion. Blood. 2007; 110(3):1036–1042. [PubMed: 17468340]
8. Ruangjirachuporn W, Udomsangpetch R, Carlsson J, Drenckhahn D, Perlmann P, Berzins K. *Plasmodium falciparum* : Analysis of the Interaction of Antigen Pf155/RESA with the Erythrocyte Membrane be associated with the micronemes. Exp Parasitol. 1991; 72(191):62–72.

9. Bennett BJ, Mohandas N, Coppel RL. Defining the minimal domain of the *Plasmodium falciparum* protein MESA involved in the interaction with the red cell membrane skeletal protein 4.1. J Biol Chem. 1997; 272(24):15299–15306. [PubMed: 9182557]
10. Lustigman S, Anders R, Brown G, Coppel R. The mature-parasite-infected erythrocyte surface antigen (MESA) of *Plasmodium falciparum* associates with the erythrocyte membrane skeletal protein, band 4.1. Mol Biochem Parasitol. 1990; 38(2):261–270. [PubMed: 2183050]
11. Waller KL, Nunomura W, An X, Cooke BM, Mohandas N, Coppel RL. Mature parasite-infected erythrocyte surface antigen (MESA) of *Plasmodium falciparum* binds to the 30-kDa domain of protein 4.1 in malaria-infected red blood cells. Blood. 2003; 102(5):1911–4. [PubMed: 12730097]
12. Waller KL, Stubberfield LM, Dubljevic V, Nunomura W, An X, Mason AJ, Mohandas N, Cooke BM, Coppel RL. Interactions of *Plasmodium falciparum* erythrocyte membrane protein 3 with the red blood cell membrane skeleton. Biochim Biophys Acta. 2007; 1768:2145–2156. [PubMed: 17570341]
13. Proellocks NI, Herrmann S, Buckingham DW, Hanssen E, Hodges EK, Elsworth B, Morahan BJ, Coppel RL, Cooke BM. A lysine-rich membrane-associated PHISTb protein involved in alteration of the cytoadhesive properties of *Plasmodium falciparum*-infected red blood cells. FASEB journal : official publication of the Federation of American Societies for Experimental Biology. 2014:1–11. [PubMed: 24385568]
14. Waller KL, Stubberfield LM, Dubljevic V, Buckingham DW, Mohandas N, Coppel RL, Cooke BM. Interaction of the exported malaria protein Pf332 with the red blood cell membrane skeleton. Biochim Biophys Acta. 2010; 1798(5):861–71. [PubMed: 20132790]
15. Rubtsov AM, Lopina OD. Ankyrins. FEBS Lett. 2000; 482:1–5. [PubMed: 11018513]
16. Lux SE. Anatomy of the red cell membrane skeleton: unanswered questions. Blood. 2016; 127(2): 187–199. [PubMed: 26537302]
17. Han BG, Nunomura W, Takakuwa Y, Mohandas N, Jap BK. Protein 4.1R core domain structure and insights into regulation of cytoskeletal organization. Nat Struct Biol. 2000; 7(10):871–875. [PubMed: 11017195]
18. Nunomura W, Takakuwa Y, Parra M, Conboy J, Mohandas N. Regulation of protein 4.1R, p55, and glycophorin C ternary complex in human erythrocyte membrane. The Journal of biological chemistry. 2000; 275(32):24540–6. [PubMed: 10831591]
19. Schischmanoff PO, Winardi R, Discher DE, Parra MK, Bicknese SE, Witkowska HE, Conboy JG, Mohandas N. Defining of the Minimal Domain of Protein 4.1 Involved in Spectrin-Actin Binding. J Biol Chem. 1995; 270(36):21243–21250. [PubMed: 7673158]
20. Anong WA, Franco T, Chu H, Weis TL, Devlin EE, Bodine DM, An X, Mohandas N, Low PS. Adducin forms a bridge between the erythrocyte membrane and its cytoskeleton and regulates membrane cohesion. Blood. 2009; 114(9):1904–12. [PubMed: 19567882]
21. Diakowski W, Grzybek M, Sikorski AF. Protein 4.1, a component of the erythrocyte membrane skeleton and its related homologue proteins forming the protein 4.1/FERM superfamily. Folia Histochem Cytobiol. 2006; 44(4):231–248. [PubMed: 17219717]
22. Chishti AH, Kim AC, Marfatia SM, Lutchman M, Hanspal M, Jindal H, Liu SC, Low PS, Rouleau GA, Mohandas N, Chasis J, Conboy JG, Gascard P, Takakuwa Y, Huang SC, Benz EJJ, Bretscher A, Fehon RG, Gusella JF, Ramesh V, Solomon F, Marchesi VT, Tsukita S, Tsukita S, Hoover KB. The FERM domain: a unique module involved in the linkage of cytoplasmic proteins to the membrane. Trends Biochem Sci. 1998; 23:281–282. [PubMed: 9757824]
23. Davis LH, Bennett V. Mapping the binding sites of human erythrocyte ankyrin for the anion exchanger and spectrin. J Biol Chem. 1990; 265(18):10589–10596. [PubMed: 2141335]
24. Nicolas V, Le Van Kim C, Gane P, Birkenmeier C, Cartron JP, Colin Y, Mouro-Chanteloup I. Rh-RhAG/ankyrin-R, a new interaction site between the membrane bilayer and the red cell skeleton, is impaired by Rh(null)-associated mutation. J Biol Chem. 2003; 278(28):25526–33. [PubMed: 12719424]
25. Bennett V. Ankyrins: Adaptors between diverse plasma membrane proteins and the cytoplasm. J Biol Chem. 1992; 267(30):8703–8706. [PubMed: 1533619]

26. Michaely P, Bennett V. The membrane-binding domain of ankyrin contains four independently folded subdomains, each comprised of six ankyrin repeats. The Journal of biological chemistry. 1993; 268(30):22703–9. [PubMed: 8226780]
27. Yasunaga M, Ipsaro JJ, Mondragon A. Structurally similar but functionally diverse ZU5 domains in human erythrocyte ankyrin. J Mol Biol. 2012; 417(4):336–50. [PubMed: 22310050]
28. Ipsaro J, Huang L, Gutierrez L, MacDonald R. Molecular epitopes of the ankyrin-spectrin interaction. Biochemistry. 2008; 47:7452–7464. [PubMed: 18563915]
29. Weng H, Guo X, Papoin J, Wang J, Coppel R, Mohandas N, An X. Interaction of *Plasmodium falciparum* knob-associated histidine-rich protein (KAHRP) with erythrocyte ankyrin R is required for its attachment to the erythrocyte membrane. Biochim Biophys Acta. 2014; 1838(1 Pt B):185–92. [PubMed: 24090929]
30. Magowan C, Nunomura W, Waller KL, Yeung J, Liang J, Van Dort H, Low PS, Coppel RL, Mohandas N. *Plasmodium falciparum* histidine-rich protein 1 associates with the band 3 binding domain of ankyrin in the infected red cell membrane. Biochimica et Biophysica Acta - Molecular Basis of Disease. 2000; 1502:461–470.
31. Téllez MDM, Matesanz F, Alcina A. The C-terminal domain of the *Plasmodium falciparum* acyl-CoA synthetases PfACS1 and PfACS3 functions as ligand for ankyrin. Mol Biochem Parasitol. 2003; 129:191–198. [PubMed: 12850263]
32. Parish LA, Mai DW, Jones ML, Kitson EL, Rayner JC. A member of the *Plasmodium falciparum* PHIST family binds to the erythrocyte cytoskeleton component band 4.1. Malar J. 2013; 12(1): 160–160. [PubMed: 23663475]
33. Vignali M, McKinlay A, LaCount DJ, Chettier R, Bell R, Sahasrabudhe S, Hughes RE, Fields S. Interaction of an atypical *Plasmodium falciparum* ETRAMP with human apolipoproteins. Malar J. 2008; 7:211. [PubMed: 18937849]
34. LaCount DJ, Vignali M, Chettier R, Phansalkar A, Bell R, Hesselberth JR, Schoenfeld LW, Ota I, Sahasrabudhe S, Kurschner C, Fields S, Hughes RE. A protein interaction network of the malaria parasite *Plasmodium falciparum*. Nature. 2005; 438(7064):103–7. [PubMed: 16267556]
35. Uetz P, Giot L, Cagney G, Mansfield Ta, Judson RS, Knight JR, Lockshon D, Narayan V, Srinivasan M, Pochart P, Qureshi-Emili a, Li Y, Godwin B, Conover D, Kalbfleisch T, Vijayadamodar G, Yang M, Johnston M, Fields S, Rothberg JM. A comprehensive analysis of protein-protein interactions in *Saccharomyces cerevisiae,* Nature. 2000; 403(February):623–627. [PubMed: 10688190]
36. LaCount, DJ. Interactome Mapping in Malaria Parasites: Challenges and Opportunities. In: Suter, B., Wanker, EE., editors. Two Hybrid Technologies. Humana Press; 2012. p. 121-145.
37. James P, Halladay J, Craig E. Genomic libraries and a host strain designed for highly efficient two-hybrid selection in yeast. Genetics. 1996; 44(4):1425–1436.
38. Aurrecoechea C, Brestelli J, Brunk BP, Dommer J, Fischer S, Gajria B, Gao X, Gingle A, Grant G, Harb OS, Heiges M, Innamorato F, Iodice J, Kissinger JC, Kraemer E, Li W, Miller JA, Nayak V, Pennington C, Pinney DF, Roos DS, Ross C, Stoeckert CJ Jr, Treatman C, Wang H. PlasmoDB: a functional genomic database for malaria parasites. Nucleic Acids Res. 2009; 37(Database issue):D539–43. [PubMed: 18957442]
39. Kilili GK, LaCount DJ. An erythrocyte cytoskeleton-binding motif in exported *Plasmodium falciparum* proteins. Eukaryotic Cell. 2011; 10(11):1439–1447. [PubMed: 21908595]
40. Brown HF, Wang L, Khadka S, Fields S, Lacount DJ. A densely overlapping gene fragmentation approach improves yeast two-hybrid screens for *Plasmodium falciparum* proteins. Mol Biochem Parasitol. 2011; 178(1–2):56–9. [PubMed: 21530591]
41. Nakayasu ES, Sobreira TJ, Torres R Jr, Ganiko L, Oliveira PS, Marques AF, Almeida IC. Improved proteomic approach for the discovery of potential vaccine targets in *Trypanosoma cruzi*. J Proteome Res. 2012; 11(1):237–46. [PubMed: 22115061]
42. Sontag RL, Nakayasu ES, Brown RN, Niemann GS, Sydor MA, Sanchez O, Ansong C, Lu SY, Choi H, Valleau D, Weitz KK, Savchenko A, Cambronne ED, Adkins JN, McFall-Ngai MJ. Identification of Novel Host Interactors of Effectors Secreted by *Salmonella* and *Citrobacter*. mSystems. 2016; 1(4):e00032–15.

43. Cox J, Mann M. MaxQuant enables high peptide identification rates, individualized p.p.b.-range mass accuracies and proteome-wide protein quantification. Nat Biotechnol. 2008; 26(12):1367–72. [PubMed: 19029910]
44. Choi H, Larsen B, Lin ZY, Breitkreutz A, Mellacheruvu D, Fermin D, Qin ZS, Tyers M, Gingras AC, Nesvizhskii AI. SAINT: probabilistic scoring of affinity purification-mass spectrometry data. Nat Methods. 2011; 8(1):70–3. [PubMed: 21131968]
45. Teo G, Liu G, Zhang J, Nesvizhskii AI, Gingras AC, Choi H. SAINTexpress: improvements and additional features in Significance Analysis of INTeractome software. J Proteomics. 2014; 100:37–43. [PubMed: 24513533]
46. Murphy HTSC, Hamm HE, Lomasney JW, Mohandas N, et al. Erythrocyte G protein as a novel target for malarial chemotherapy. PLoS Med. 2006; 3(12)
47. Lavazec C, Deplaine G, Safeukui I, Perrot S, Milon G, Mercereau-Puijalon O, David PH, Buffet P. Microsphiltration: a microsphere matrix to explore erythrocyte deformability. Methods Mol Biol. 2013; 923:291–7. [PubMed: 22990786]
48. Stelzl U, Worm U, Lalowski M, Haenig C, Brembeck FH, Goehler H, Stroedicke M, Zenkner M, Schoenherr A, Koeppen S, Timm J, Mintzlaff S, Abraham C, Bock N, Kietzmann S, Goedde A, Toksoz E, Droege A, Krobitsch S, Korn B, Birchmeier W, Lehrach H, Wanker EE. A human protein-protein interaction network: a resource for annotating the proteome. Cell. 2005; 122(6): 957–68. [PubMed: 16169070]
49. Chen YC, Rajagopala SV, Stellberger T, Uetz P. Exhaustive benchmarking of the yeast two-hybrid system. Nat Methods. 2010; 7(9):667–8. author reply 668. [PubMed: 20805792]
50. Sargeant TJ, Marti M, Caler E, Carlton JM, Simpson K, Speed TP, Cowman AF. Lineage-specific expansion of proteins exported to erythrocytes in malaria parasites. Genome Biol. 2006; 7(2):R12. [PubMed: 16507167]
51. Warncke JD, Vakonakis I, Beck HP. *Plasmodium* Helical Interspersed Subtelomeric (PHIST) Proteins, at the Center of Host Cell Remodeling. Microbiol Mol Biol Rev. 2016; 80(4):905–27. [PubMed: 27582258]
52. Oakley MS, Kumar S, Anantharaman V, Zheng H, Mahajan B, Haynes JD, Moch JK, Fairhurst R, McCutchan TF, Aravind L. Molecular factors and biochemical pathways induced by febrile temperature in intraerythrocytic *Plasmodium falciparum* parasites. Infect Immun. 2007; 75(4): 2012–25. [PubMed: 17283083]
53. Frech C, Chen N. Variant Surface antigens of malaria parasites: functional and evolutionary insights from comparative gene family classification and analysis. BMC Genomics. 2013; 14
54. Kats LM, Proellocks NI, Buckingham DW, Blanc L, Hale J, Guo X, Pei X, Herrmann S, Hanssen EG, Coppel RL, Mohandas N, An X, Cooke BM. Interactions between *Plasmodium falciparum* skeleton-binding protein 1 and the membrane skeleton of malaria-infected red blood cells. Biochim Biophys Acta. 2015; 1848(7):1619–28. [PubMed: 25883090]
55. Sharma S, Zingde SM, Gokhale SM. Identification of human erythrocyte cytosolic proteins associated with plasma membrane during thermal stress. J Membr Biol. 2013; 246(8):591–607. [PubMed: 23774970]
56. Mantel PY, Hjelmqvist D, Walch M, Kharoubi-Hess S, Nilsson S, Ravel D, Ribeiro M, Gruring C, Ma S, Padmanabhan P, Trachtenberg A, Ankarklev J, Brancucci NM, Huttenhower C, Duraisingh MT, Ghiran I, Kuo WP, Filgueira L, Martinelli R, Marti M. Infected erythrocyte-derived extracellular vesicles alter vascular function via regulatory Ago2-miRNA complexes in malaria. Nat Commun. 2016; 7:12727. [PubMed: 27721445]
57. Mantel PY, Hoang AN, Goldowitz I, Potashnikova D, Hamza B, Vorobjev I, Ghiran I, Toner M, Irimia D, Ivanov AR, Barteneva N, Marti M. Malaria-infected erythrocyte-derived microvesicles mediate cellular communication within the parasite population and with the host immune system. Cell Host Microbe. 2013; 13(5):521–34. [PubMed: 23684304]
58. Maier AG, Rug M, O'Neill MT, Brown M, Chakravorty S, Szestak T, Chesson J, Wu Y, Hughes K, Coppel RL, Newbold C, Beeson JG, Craig A, Crabb BS, Cowman AF. Exported proteins required for virulence and rigidity of *Plasmodium falciparum*-infected human erythrocytes. Cell. 2008; 134(1):48–61. [PubMed: 18614010]

59. Pei X, Guo X, Coppel R, Mohandas N, An X. *Plasmodium falciparum* erythrocyte membrane protein 3 (PfEMP3) destabilizes erythrocyte membrane skeleton. The Journal of biological chemistry. 2007; 282(37):26754–8. [PubMed: 17626011]
60. Sanyal S, Egee S, Bouyer G, Perrot S, Safeukui I, Bischoff E, Buffet P, Deitsch KW, Mercereau-Puijalon O, David PH, Templeton TJ, Lavazec C. *Plasmodium falciparum* STEVOR proteins impact erythrocyte mechanical properties. Blood. 2012; 119(2):e1–8. [PubMed: 22106347]
61. Diez-Silva M, Park Y, Huang S, Bow H, Mercereau-Puijalon O, Deplaine G, Lavazec C, Perrot S, Bonnefoy S, Feld MS, Han J, Dao M, Suresh S. Pf155/RESA protein influences the dynamic microcirculatory behavior of ring-stage *Plasmodium falciparum* infected red blood cells. Scientific reports. 2012; 2:614. [PubMed: 22937223]
62. Deplaine G, Safeukui I, Jeddi F, Lacoste F, Brousse V, Perrot S, Biligui S, Guillotte M, Guitton C, Dokmak S, Aussilhou B, Sauvanet A, Cazals Hatem D, Paye F, Thellier M, Mazier D, Milon G, Mohandas N, Mercereau-Puijalon O, David PH, Buffet Pa. The sensing of poorly deformable red blood cells by the human spleen can be mimicked in vitro. Blood. 2011; 117(8):e88–95. [PubMed: 21163923]
63. Pei X, Guo X, Coppel R, Bhattacharjee S, Haldar K, Gratzer W, Mohandas N, An X. The ring-infected erythrocyte surface antigen (RESA) of *Plasmodium falciparum* stabilizes spectrin tetramers and suppresses further invasion. Blood. 2007
64. Pei X, Guo X, Coppel R, Mohandas N, An X. *Plasmodium falciparum* Erythrocyte Membrane Protein 3 (PfEMP3) Destabilizes Erythrocyte Membrane Skeleton. J Biol Chem. 2007; 282(37): 26754–8. [PubMed: 17626011]
65. Walensky, LD., Mohandas, N., Lux, SE. Disorders of the Red Blood Cell Membrane. In: Handin, RI.Lux, SE., Stossel, TP., editors. Blood: Principles and Practce of Hematology. Lippincott Williams & Wilkins; Philadelphia: 2003. p. 1709-1858.
66. Murphy SC, Harrison T, Hamm HE, Lomasney JW, Mohandas N, Haldar K. Erythrocyte G protein as a novel target for malarial chemotherapy. PLoS Med. 2006; 3(12):e528. [PubMed: 17194200]
67. Otto TD, Wilinski D, Assefa S, Keane TM, Sarry LR, Bohme U, Lemieux J, Barrell B, Pain A, Berriman M, Newbold C, Llinas M. New insights into the blood-stage transcriptome of *Plasmodium falciparum* using RNA-Seq. Mol Microbiol. 2010; 76(1):12–24. [PubMed: 20141604]
68. Bertin GI, Sabbagh A, Argy N, Salnot V, Ezinmegnon S, Agbota G, Laipo Y, Alao JM, Sagabo G, Guillonneau F, Deloron P. Proteomic analysis of *Plasmodium falciparum* parasites from patients with cerebral and uncomplicated malaria. Sci Rep. 2016; 6
69. Atkinson CT, Aikawa M, Perry G, Fujino T, Bennett V, Davidson EA, Howard RJ. Ultrastructural localization of erythrocyte cytoskeletal and integral membrane proteins in *Plasmodium falciparum*-infected erythrocytes. European J Cell Bio. 1987; 45:192–199.
70. Nunomura W, Gascard P, Takakuwa Y. Insights into the function of the unstructured N-terminal domain of proteins 4.1R and 4.1G in erythropoiesis. Int J Cell Biol. 2011 2011(Figure 2).
71. Gimm JA, An X, Nunomura W, Mohandas N. Functional characterization of spectrin-actin-binding domains in 4.1 family of proteins. Biochemistry. 2002; 41:7275–7282. [PubMed: 12044158]
72. An X, Takakuwa Y, Nunomura W, Manno S, MN. Modulation of Band 3-Ankyrin Interaction by Protein 4.1. J Biol Chem. 1996
73. Low PS, Willardson BM, Mohandas N, Rossi M, Shohet S. Contribution of the Band 3-Ankyrin Interaction to Erythrocyte Membrane Mechanical Stability. Blood. 1991; 77(7):1581–1586. [PubMed: 1826225]
74. Tarr SJ, Moon RW, Hardege I, Osborne AR. A conserved domain targets exported PHISTb family proteins to the periphery of *Plasmodium* infected erythrocytes. Mol Biochem Parasitol. 2014; 196(1):29–40. [PubMed: 25106850]

Highlights

- Identified eight exported *P. falciparum* proteins that bound to ankyrin or band 4.1.
- PF3D7_0402000 (PFD0090c) bound to both ankyrin and band 4.1
- PF3D7_0402000 reduced migration of erythrocyte ghosts through a microsphere matrix.

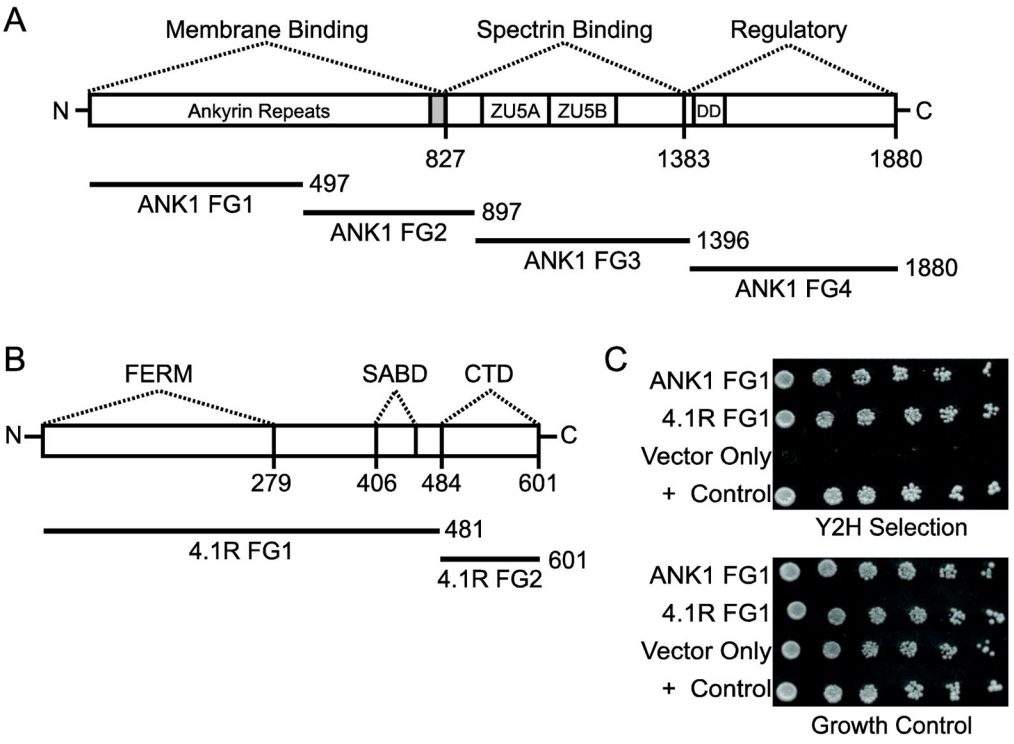

Fig. 1. PF3D7_0402000 (D90c) interacts with ankyrin and 4.1R in the Y2H assay

Protein domains of (A) human erythrocyte ankyrin (ANK1) and (B) band 4.1 (4.1R) are indicated above bars representing each protein. ZU5A and ZU5B correspond to the zona occludens 1 (ZO-1) protein/unc5-like netrin receptor domains; FERM, the Four-point-one, Ezrin, Radixin, Moesin domain (also referred to as the 4.1R 30 kDa domain); DD, the death domain; SABD, the spectrin-actin-binding domain; and CTD, the C-terminal domain. Solid bars represent the four ankyrin (ANK1 FG1–4) and two 4.1R fragments used in the Y2H assay. ANK1 FG1 and FG2 contain ankyrin repeats 1–14 and 15–24, respectively. The shaded region indicates hinge region following ankyrin repeats. Numbers indicate amino acid positions. (C) Pairwise Y2H assays of human erythrocyte ankyrin (ANK1 FG1) and band 4.1 (4.1R FG1) with D90c. Five-fold serial dilutions of diploid yeast expressing D90c as a fusion to the Gal4 DNA binding domain (DBD) and ankyrin or 4.1R fragments as fusions to the Gal4 activation domain (AD) were plated on growth medium lacking tryptophan and leucine (to show equal amounts of yeast) and Y2H selection medium lacking tryptophan, leucine, uracil and histidine supplemented with 1 mM 3-amino-1,2,4-triazole and incubated for 7 days. “Vector only” indicates negative control diploid yeast expressing empty AD + DBD-D90c. Diploids containing PFE1350c and PFC0255c were included as a positive (+) control [34, 40].

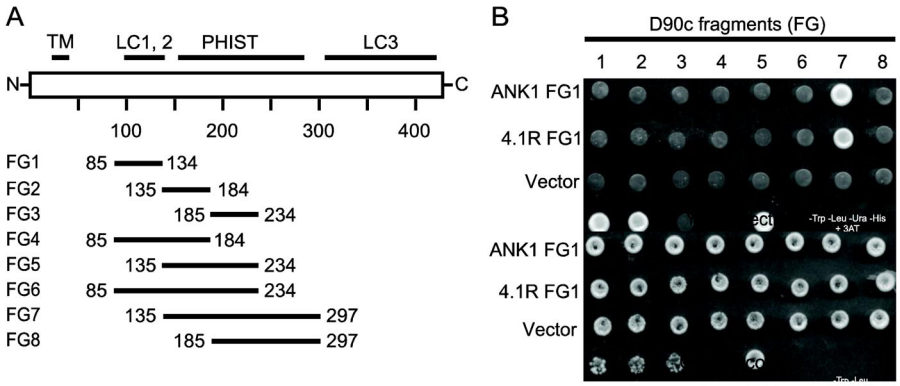

Fig. 2. The PF3D7_0402000 (D90c) PHIST domain is required for interaction with ankyrin and 4.1R

A) A series of PF3D7_0402000 (D90c) deletion constructs were used to define the smallest region capable of interacting with ANK1 FG1 and 4.1R FG1. The diagram shows the domain organization of D90c (white bar) and fragments (solid bars) used to map the minimum binding region. TM indicates predicted transmembrane domain; LC, low complexity region; PHIST, Poly-Helical Interspersed Sub-Telomeric domain. Numbers indicate amino acid positions. B) Pairwise Y2H assays of ANK1 FG1 and 4.1R FG1 with eight deletion constructs of D90c. Diploid yeast expressing D90c fragments as a fusion to the Gal4 AD and ankyrin or 4.1R fragments as fusions to the Gal4 DBD were plated on growth medium lacking tryptophan and leucine (to show equal amounts of yeast) (bottom panel) and Y2H selection medium lacking tryptophan, leucine, uracil and histidine supplemented with 1 mM 3-amino-1,2,4-triazole (top panel). The numbers above the top panel indicate the name of D90c fragments. “Vector only” indicates negative control diploid yeast expressing empty AD + DBD-D90c.

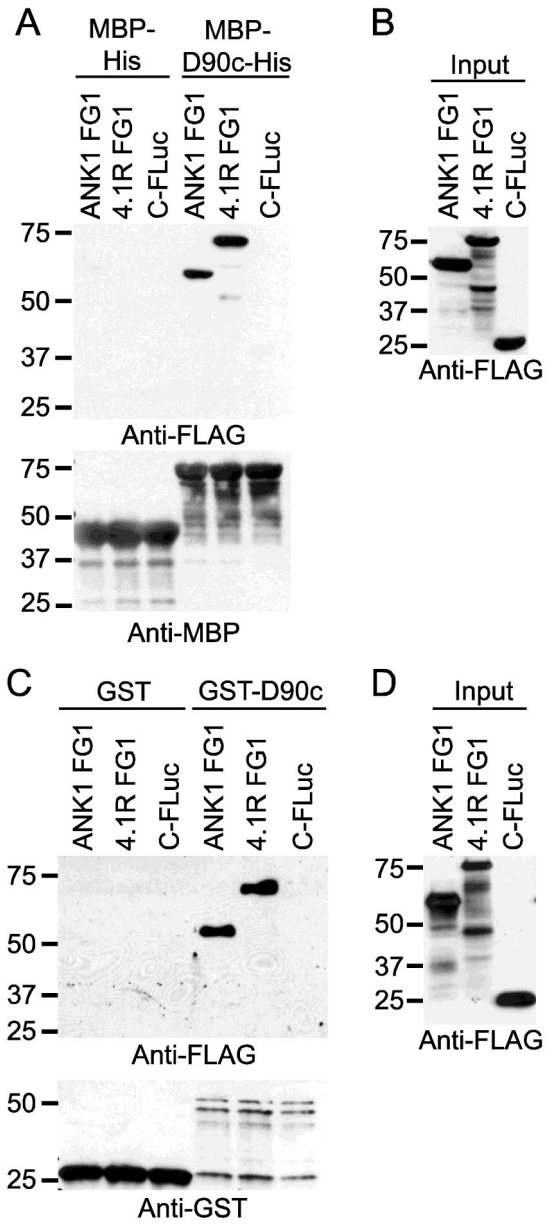

Fig. 3. PF3D7_0402000 (D90c) interacts with ANK1 and 4.1R in co-precipitation assays

A) and C) Expression of proteins tagged with C-terminal fragment of firefly luciferase protein (C-FLuc) and 3XFLAG. ANK1 FG1 and 4.1R FG1 as fusions to C-FLuc-3XFLAG and C-FLuc-3XFLAG with no insert were *in vitro* translated in wheat germ extracts (WGE) and subjected to western blotting with anti-FLAG tag antibody. Molecular weight markers (sizes in kDa) are indicated at left. B) Co-affinity purification of erythrocyte ankyrin and 4.1R with MBP-His-tagged PF3D7_0402000 (MBP-D90c-His). C-FLuc-3XFLAG-tagged proteins from (A) were incubated with MBP-D90c-His and MBP-His and purified with amylose resin. The co-purifying proteins were subjected to SDS-PAGE analysis and western blotting using anti-FLAG antibody (top panel) and anti-MBP antibody (bottom panel). Molecular weight markers (sizes in kDa) are indicated at left. D) Co-affinity purification of

erythrocyte ankyrin and 4.1R with GST tagged-PF3D7_0402000 (GST-D90c). GST and GST-D90c were *in vitro* translated in WGE, incubated with C-FLuc-3XFLAG-tagged proteins from (C) and purified with GST beads. The co-purifying proteins were subjected to SDS-PAGE and western blotting using anti-FLAG (top panel) and anti-GST antibodies (bottom panel). Molecular weight markers (sizes in kDa) are indicated at left.

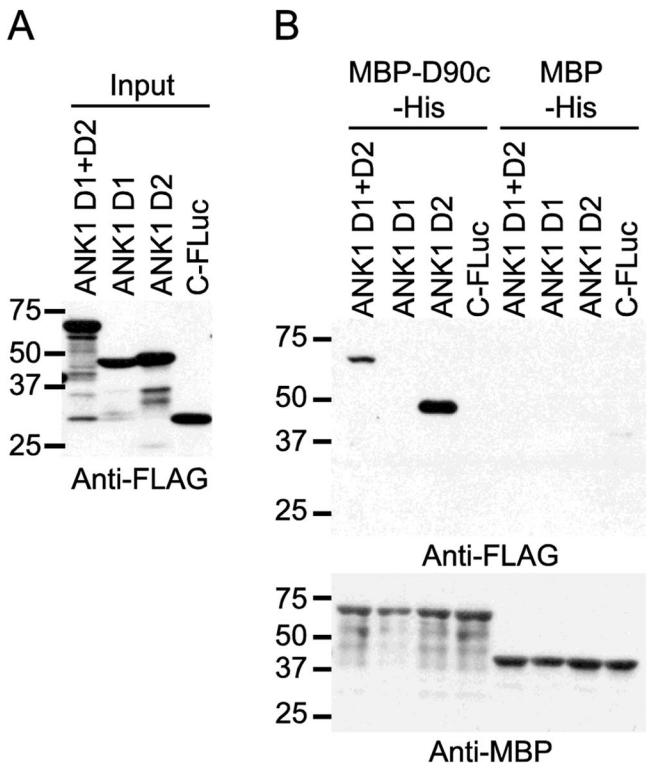

Fig. 4. PF3D7_0402000 (D90c) targets the 2nd folding domain of ANK1

A) Expression of proteins tagged with the C-terminal fragment of firefly luciferase protein (C-FLuc) and 3XFLAG. D1, D2 and D1+D2 subdomains of ANK1 as fusions to C-FLuc-3XFLAG and C-FLuc-3XFLAG with no insert were in vitro translated in wheat germ extracts (WGE) and subjected to SDS-PAGE and western blotting with anti-FLAG tag antibody. Molecular weight markers (sizes in kDa) are indicated at left. B) Co-affinity purification of ANK1 subdomains with MBP-D90c-His. C-FLuc-3XFLAG-tagged proteins from (A) were incubated with MBP-D90c-His and MBP-His and purified with amylose resin. The co-purifying proteins were subjected to SDS-PAGE and western blotting using anti- FLAG (top panel) and anti-MBP antibodies (bottom panel). Molecular weight markers (sizes in kDa) are indicated at left.

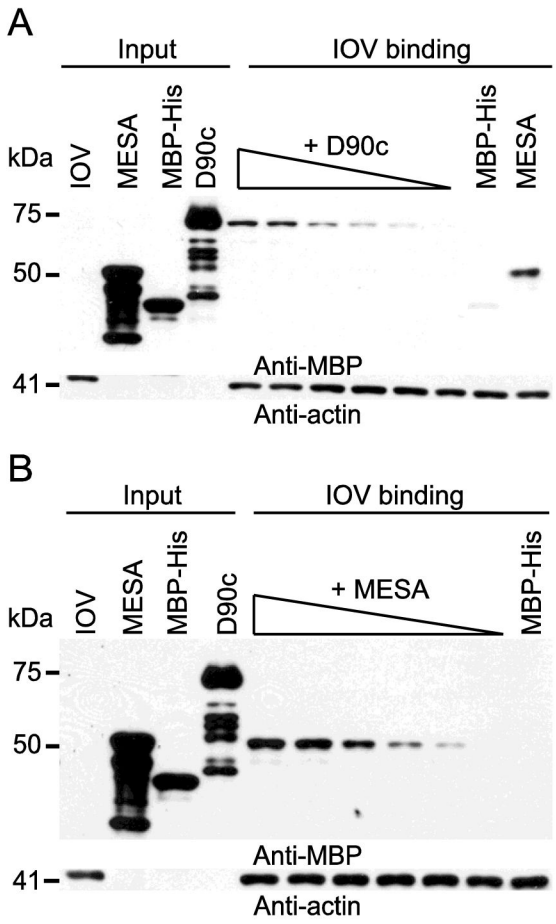

Fig. 5. PF3D7_0402000 (D90c) binds to inside out vesicles (IOVs) in a concentration-dependent manner

Western blots of IOV binding assay for A) D90c and B) Mature parasite-infected erythrocyte surface antigen (MESA). *E. coli*-expressed purified proteins, MBP-D90c-His and MBP-MESA at concentrations ranging from 0.0008 μM to 0.023 μM were separately incubated overnight with 10 μg of erythrocyte IOVs, collected by centrifugation, washed, and subjected to SDS-PAGE analysis and western blotting using anti-MBP antibody. Blots were reprobed with anti-actin antibody to demonstrate equal loading. MESA and MBP-His protein were included as positive and negative controls, respectively. Molecular weight markers (sizes in kDa) are indicated at left.

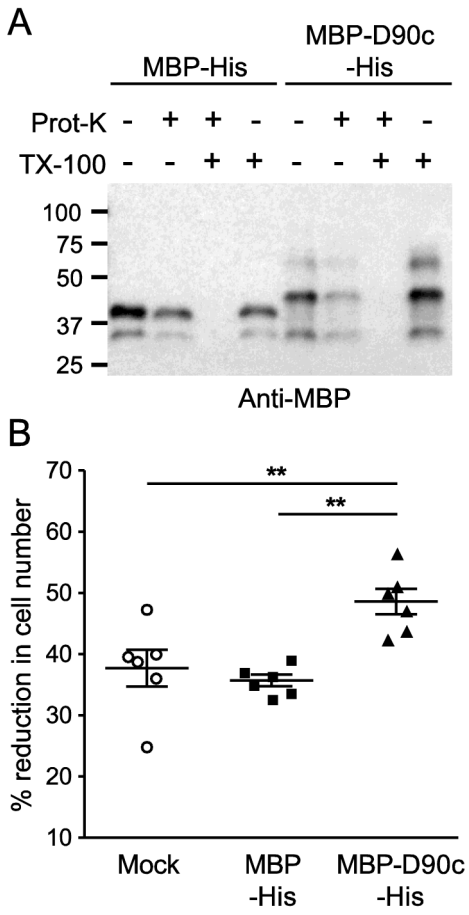

Fig. 6. PF3D7_0402000 (D90c) reduces the passage of erythrocyte ghosts through a microsphere matrix

Erythrocyte ghosts loaded with MBP-His or MBP-D90c-His (30 μM each) or mock-treated. A) Proteinase protection assay. Erythrocyte ghosts were loaded with MBP-His or MBP-D90c-His, mock treated or treated with 100 μg/ml of Proteinase K, 0.5% Triton X-100 or both, and subjected to western blotting with an anti-MBP antibody. B) Microsphiltration of MBP-His- and MBP-D90c-His-loaded erythrocyte ghost cells. Loaded erythrocyte ghosts were passed through a microsphere matrix and the number of erythrocytes in the upstream and downstream samples were quantitated by hemocytometer. Graph shows the percent reduction in cell number in the downstream samples. Statistical significance was determined by using the Mann-Whitney U test (**P<0.01).

Table 1

P. falciparum exported proteins that interacted with ANK1 and 4.1R in yeast two-hybrid screens

Bait	Prey (former name)	Description
ANK1 FG3	PF3D7_0115000 (PFA0725w)	SURFIN 1.3
ANK1 FG3	PF3D7_1149200 (PF11_0509)	RESA
ANK1 FG3	PF3D7_0800700 (MAL8P1.162)	SURFIN 8.3
ANK1 FG3	PF3D7_0500800 (PFE0040c)	MESA
ANK1 FG3	PF3D7_0902700 (PFI0130c)	PHISTb protein
4.1R FG1	PF3D7_0402000 (PFD0090c)	PHISTa protein
4.1R FG2	PF3D7_1102500 (PF11_0037)	PHISTb protein
4.1R FG2	PF3D7_0402200 (PFD0100c)	SURFIN 4.1

Table 2

Identification or erythrocyte proteins that bound to PF3D7_0402000 by co-affinity purification plus mass spectrometry

Protein Name	Gene Name	Spectral Counts*	Control Spectral Counts*	Fold Enrichment**	Saint Score	BFDR ***
W4J5J2	PF3D7_0402000	248|182	0|1	430	1	0
P11171	EPB41	145|160	27|22	6.22	1	0
P16157	ANK1	36|15	0|0	255	1	0
P04406	GAPDH	28|22	0|2	25	1	0
P68871	HBB	16|8	0|0	120	1	0
P04040	CAT	19|4	0|1	23	1	0
P16452	EPB42	10|12	0|0	110	1	0
Q08495	DMTN	10|9	1|1	9.5	1	0
P69905	HBA1	12|4	1|1	8	0.99	0
Q00577	PURA	7|7	0|0	70	1	0
Q9UKV8	AGO2	5|5	0|0	50	1	0
P11166	SLC2A1	3|5	0|0	40	1	0
P02730	SLC4A1	3|4	0|0	35	1	0
P60709	ACTB	4|2	1|1	3	0.93	0
P11142	HSPA8	3|3	0|0	30	1	0
P16403	HIST1H1C	2|3	1|1	2.5	0.92	0.01

*Spectral counts from two replicates are shown (Replicate 1|Replicate 2)

**Fold enrichment was calculated by dividing the average of the spectral counts from the MBP-PF3D7_0402000 co-purification by that of the MBP-His co-purification. If the prey protein was not detected in the MBP-His co-purification, the average spectral counts from the MBP-PF3D7_0402000 co-purification was divided by 0.1.

***BFDR, Bayesian False Discovery Rate